SUPPORTING INFORMATION

Electrocatalytic Valorization of 5-Hydroxymethylfurfural Coupling with Hydrogen Production by Tetraruthenium-Containing Polyoxometalate-based Composite

Hui Zhou,[a] Yuanyuan Dong,*[a] Xing Xin,[a] Manzhou Chi,[a] Tinglu Song,[b] and Hongjin Lv*[a]

[a] *MOE Key Laboratory of Cluster Science, School of Chemistry and Chemical Engineering, Beijing Institute of Technology, Beijing 102488, P. R. China.*
[b] *Experimental Center of Advanced Materials School of Materials Science & Engineering，Beijing Institute of Technology.*

Table of content

1. Figure S1-S13

Figure S1. Optical photo of the aqueous solution of the **Ru_4**-containg residue after TG analysis. ····· 3

Figure S2. SEM image of **Ru_4**/PEI-rGO. ····· 3

Figure S3. Energy-dispersive X-ray (EDX) elements analysis of **Ru_4**/PEI-rGO. ····· 3

Figure S4. The survey XPS spectra of **Ru_4** and **Ru_4**/PEI-rGO. ····· 4

Figure S5. HPLC spectra of the anode oxidation products for **Ru_4**/PEI-rGO electrocatalysts. ····· 4

Figure S6. GC spectra of air and the gas products at anode chambers for rGO and PEI-rGO electrocatalysts. ····· 5

Figure S7. The electrocatalytic activities of **Ru_4**/PEI-rGO with the variation in the amount of **Ru_4**. ····· 5

Figure S8. CV curves of **Ru_4** homogeneous aqueous solution in pH 6 without and with HMF. ····· 6

Figure S9. CV curves of **Ru_4** homogeneous aqueous solution in pH 4 without and with HMF. ····· 6

Figure S10. CV curves of **Ru_4** homogeneous aqueous solution in pH 8 without and with HMF. ····· 7

Figure S11. The high resolution (a) C 1s + Ru 3d, (b) O 1s XPS spectra of fresh **Ru_4**/PEI-rGO electrocatalyst. ····· 7

Figure S12. The high resolution Ru 3p XPS spectra of **Ru_4**/PEI-rGO after reaction over 6 h at applied voltage of 0.6 V and 0.8 V at pH 6 electrolyte aolution, and pH 4 and pH 8 electrolyte at 0.94 V. ····· 8

Figure S13. The plots of the conversion of HMF and the yields of furanic products versus the electrolysis time at applied voltage of 0.94 V under pH 6 electrolyte solution with 0.6 eq. TEMPO additive. ····· 8

Figure S14. I-t response curve for **Ru_4**/PEI-rGO electrocatalyst at applied voltage of 0.94 V for 12 hours under pH 6 electrolyte solution. ····· 9

Figure S15. SEM and TEM images of **Ru_4**/PEI-rGO after bulk electrolysis for 12 hours. ····· 9

2. Table S1-S2

Table S1. The electrocatalytic activities of **Ru_4**/PEI-rGO catalysts with the different amount of PEI. ····· 9

Table S2. The electrocatalytic activities of **Ru_4**/PEI-rGO catalysts with the different loading quantity of the composite electrocatalyst onto carbon cloth. ····· 10

Table S3. Comparation of the electrocatalytic oxidation of HMF to DFF using different noble metal-based electrocatalysts. ····· 10

1. Figure S1-S13

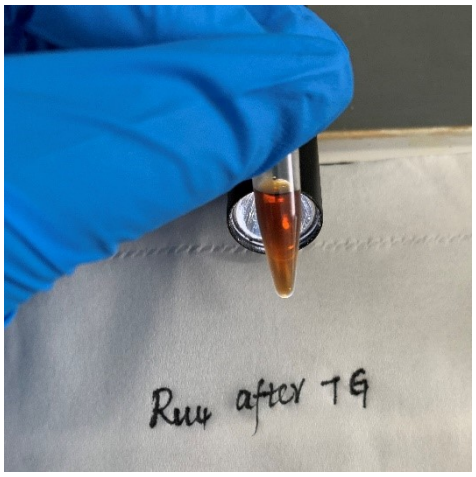

Figure S1 Optical photo of the aqueous solution of the **Ru$_4$**-containg residue after TG analysis.

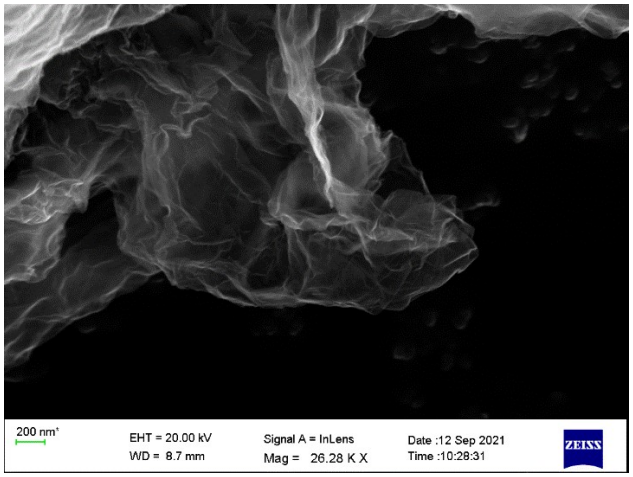

Figure S2 SEM image of **Ru$_4$**/PEI-rGO.

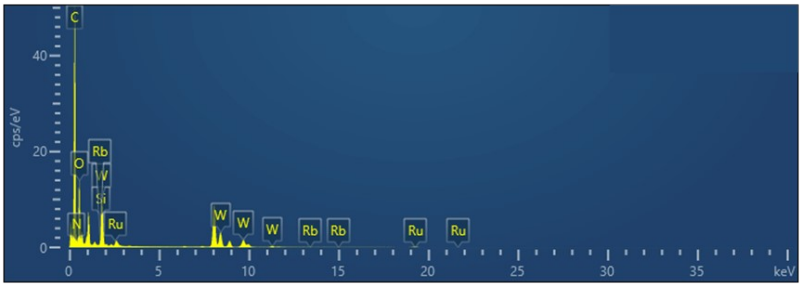

Figure S3 Energy-dispersive X-ray (EDX) elements analysis of **Ru$_4$**/PEI-rGO.

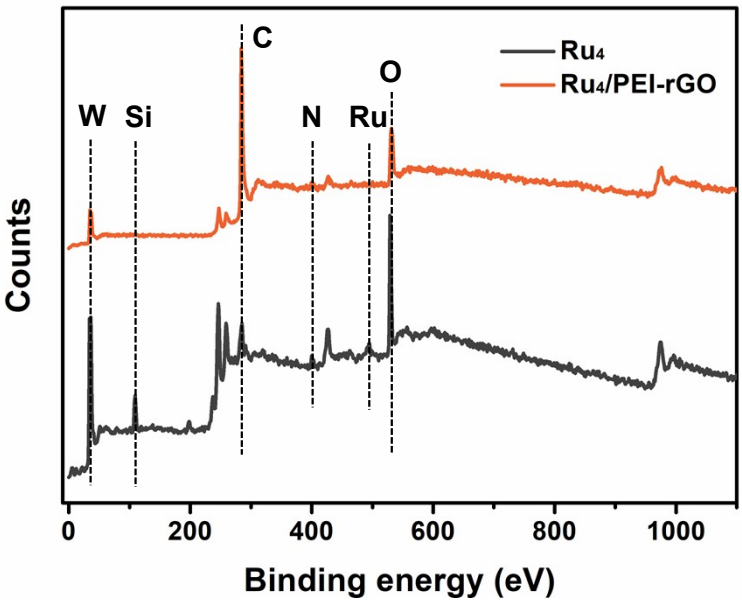

Figure S4 The survey XPS spectra of **Ru$_4$** and **Ru$_4$**/PEI-rGO.

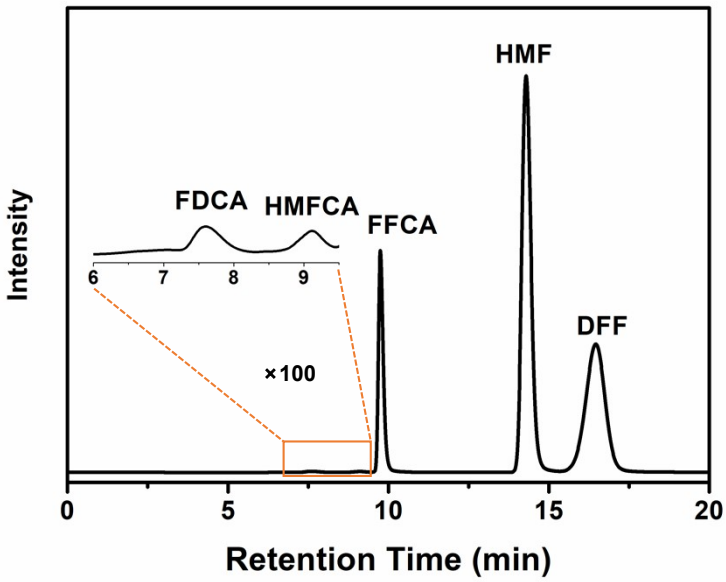

Figure S5 HPLC spectra of the anode oxidation products for **Ru$_4$**/PEI-rGO electrocatalysts.

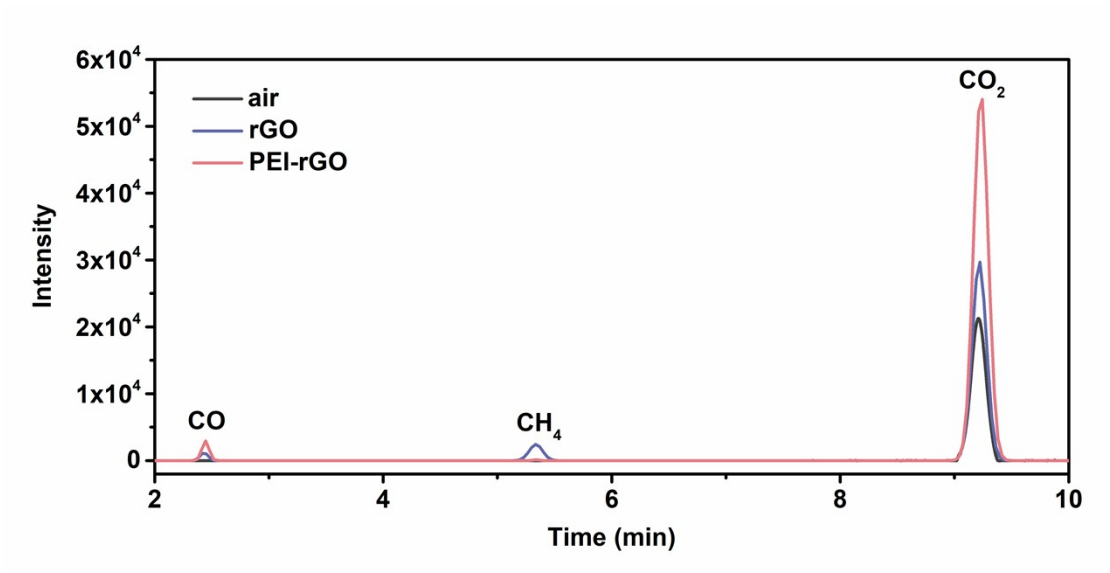

Figure S6 GC spectra of air and the gas products at anode chambers for rGO and PEI-rGO electrocatalysts.

Upon 6-hour bulk electrocatalysis for rGO and PEI-rGO, the gaseous products at the anode chambers was tested using GC. The results indicated that there were large amount of CO_2 and small amount of CO/CH_4, which fully confirmed the deep mineralization of HMF during bulk electrocatalysis for rGO and PEI-rGO electrocatalysts.

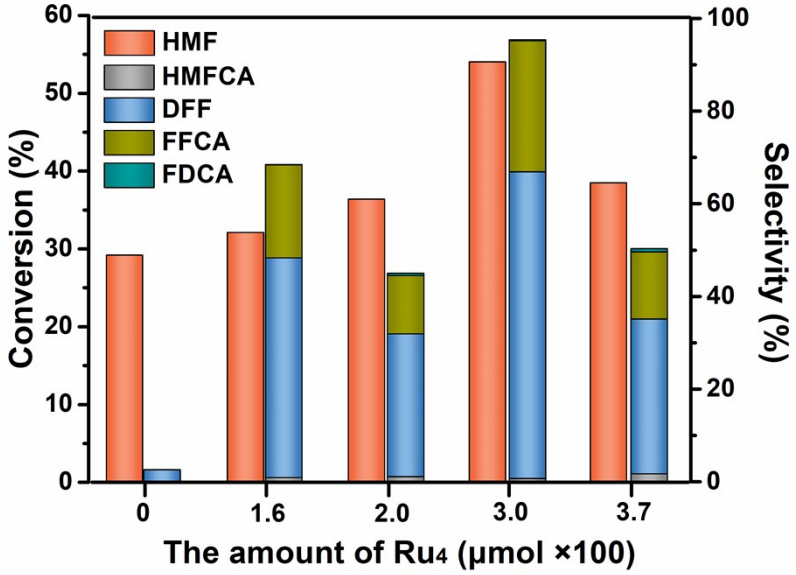

Figure S7 The electrocatalytic activities of **Ru$_4$**/PEI-rGO with the variation in the amount of **Ru$_4$**.

The amounts of **Ru$_4$** for **Ru$_4$**/PEI-rGO electrocatalysts were determined by ICP. With the amount of **Ru$_4$** increasing, the conversion of HMF and the selectivity of oxidation products displayed the shape of volcano. The optimized amount of **Ru$_4$** is 0.03 μmol, corresponding to the concentration of **Ru$_4$** aqueous solution of 1 mg/mL

during the preparation described in experimental section.

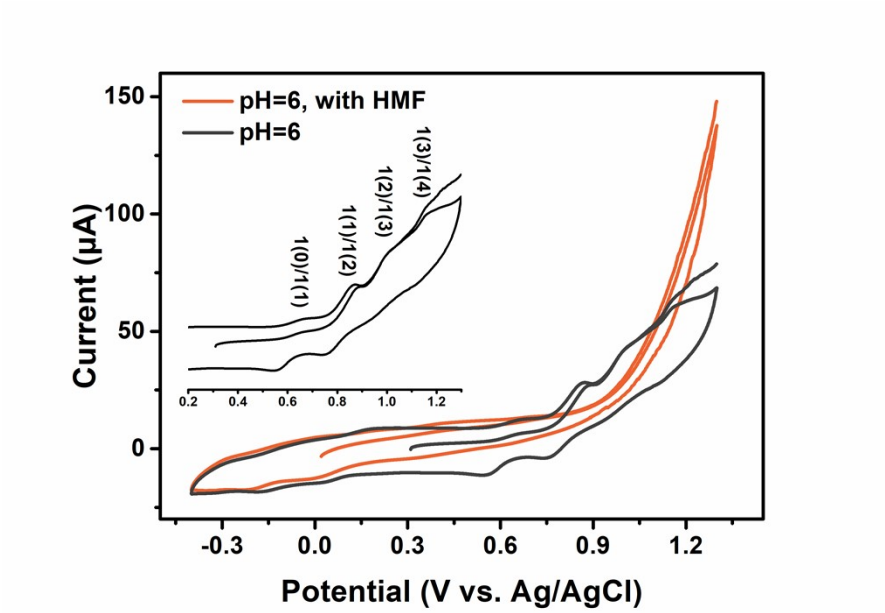

Figure S8 CV curves of **Ru$_4$** homogeneous aqueous solution in pH 6 without and with HMF.

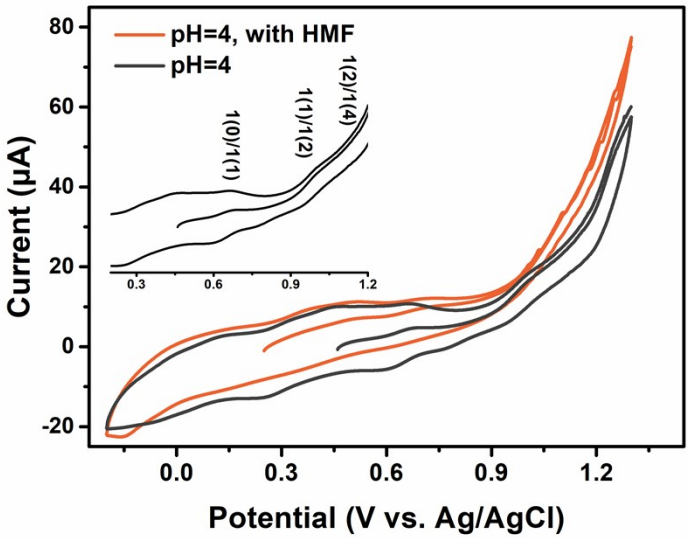

Figure S9 CV curves of **Ru$_4$** homogeneous aqueous solution in pH 4 without and with HMF.

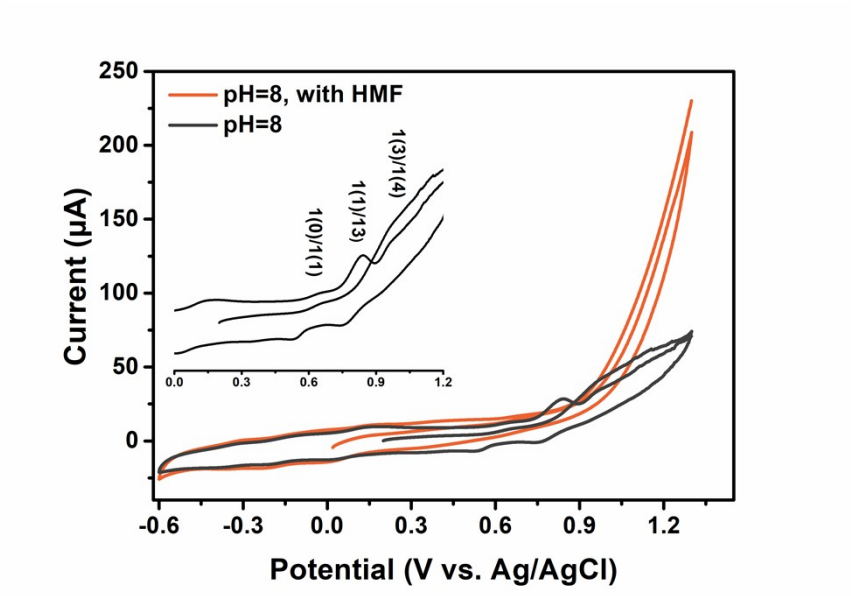

Figure S10 CV curves of **Ru$_4$** homogeneous aqueous solution in pH 8 without and with HMF.

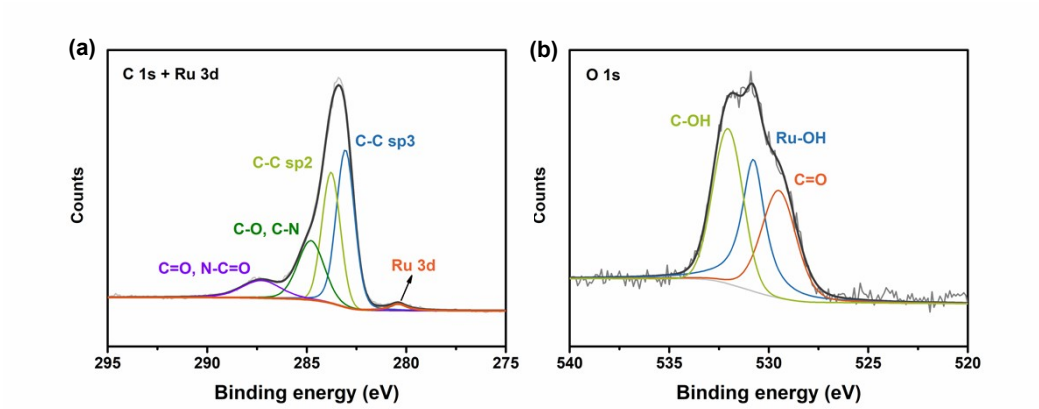

Figure S11 The high resolution (a) C 1s + Ru 3d, (b) O 1s XPS spectra of fresh **Ru$_4$**/PEI-rGO electrocatalyst.

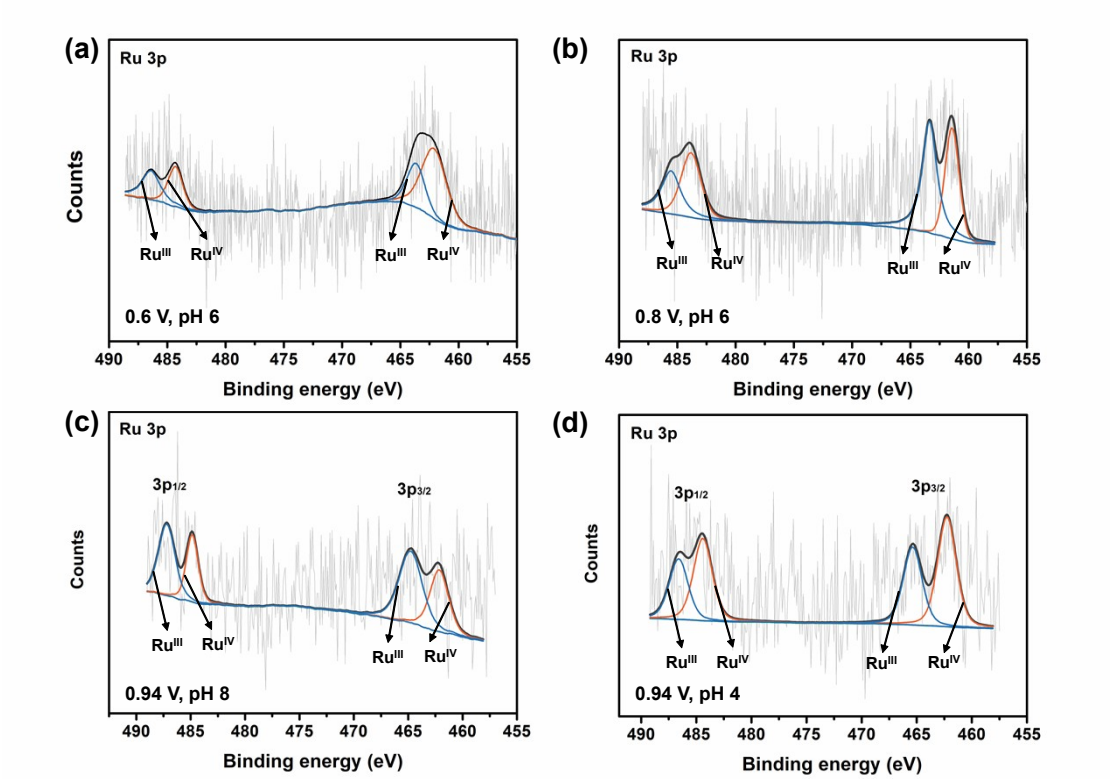

Figure S12 The high resolution XPS spectra of **Ru$_4$**/PEI-rGO after reaction over 6-hour at applied voltage of (a) 0.6 V and (b) 0.8 V at pH 6 electrolyte aolution, and (c) pH 8 and (d) pH 4 electrolyte at 0.94 V.

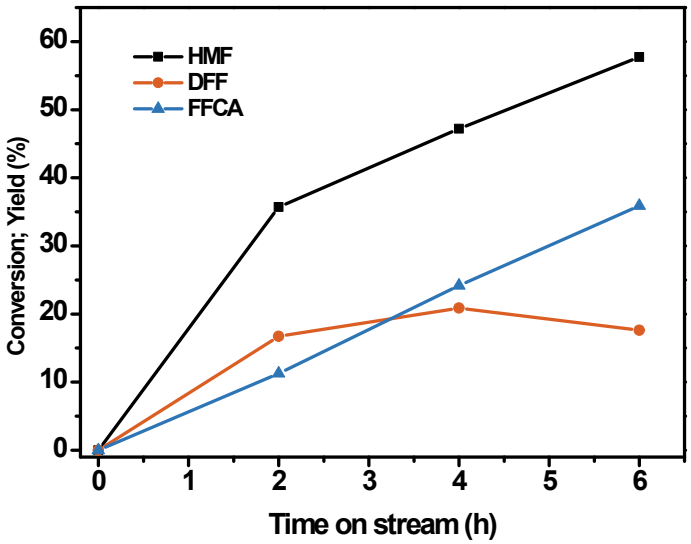

Figure S13 The plots of the conversion of HMF and the yields of furanic products versus the electrolysis time at applied voltage of 0.94 V under pH 6 electrolyte solution with 0.6 eq. TEMPO additive.

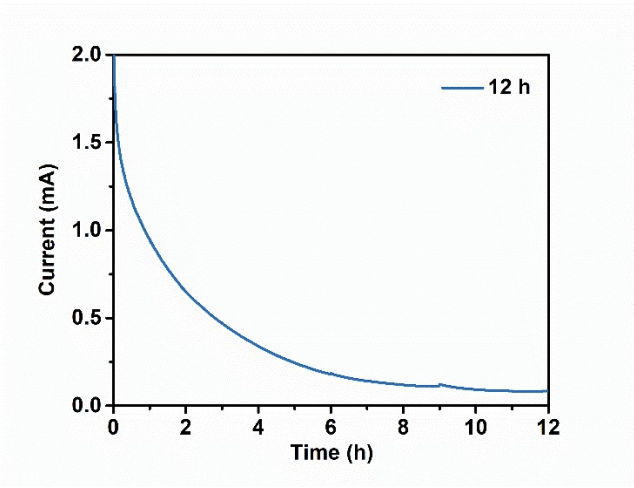

Figure S14 I-t response curve for **Ru$_4$**/PEI-rGO electrocatalyst at applied voltage of 0.94 V for 12 hours under pH 6 electrolyte solution.

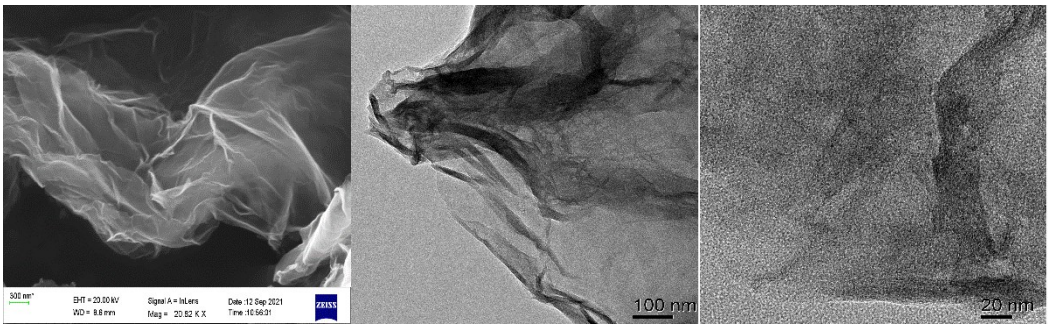

Figure S15 SEM (a) and TEM (b-c) images of **Ru$_4$**/PEI-rGO after bulk eletrolysis for 12 hours.

2. Table S1-S2

Table S1 The electrocatalytic activities of **Ru$_4$**/PEI-rGO catalysts with the different amount of PEI.

C_{PEI}[a] (mg/mL)	HMF	HMFCA		DFF		FFCA		FDCA	
	Con.	Yie.	Sel.	Yie.	Sel.	Yie.	Sel.	Yie.	Sel.
0	16.4%	0.80%	4.90%	3.66%	22.39%	1.88%	11.48%	0.36%	2.18%
4	22.4%	1.26%	5.62%	3.46%	15.49%	1.56%	6.97%	0.24%	1.07%
10	13.0%	0.63%	4.86%	0.99%	7.57%	0.40%	3.07%	-	-
50	5.2%	0.38%	7.32%	1.52%	29.12%	0.22%	4.26%	-	-

Conditions: 0.5 M HAC/NaAc buffer solution (pH 6, 40 ml), HMF (5 mM), **Ru$_4$**/PEI-rGO catalysts (0.5 mg) with different amount of PEI, reaction time (2 h), applied potential at 1.5 V vs RHE. [a] The original concentration of the PEI aqueous solution used in the **Ru$_4$**/PEI-rGO catalyst preparation process.

Table S2 The electrocatalytic activities of **Ru$_4$**/PEI-rGO catalysts with the different loading quantity of the composite electrocatalyst onto carbon cloth.

Cat.[a]	HMF	HMFCA		DFF		FFCA		FDCA	
(mg)	Con.	Yie.	Sel.	Yie.	Sel.	Yie.	Sel.	Yie.	Sel.
0.25	31.5%	0.3%	1.0%	2.3%	7.3%	0.5%	1.6%	-	-
0.37	33.6%	0.3%	1.0%	5.9%	17.4%	1.4%	4.2%	0.1%	0.2%
0.50	50.8%	0.4%	0.7%	33.6%	66.2%	14.4%	28.3%	0.1%	0.3%
0.62	35.7%	0.3%	1.0%	7.2%	20.2%	2.1%	5.8%	0.1%	0.4%
0.75	42.1%	0.5%	1.2%	16.1%	38.2%	6.2%	14.8%	0.3%	0.7%
1.00	36.3%	0.5%	1.6%	8.2%	22.5%	2.8%	7.6%	0.2%	0.5%

Conditions: 0.5 M HAc/NaAc buffer solution (pH 6, 20 ml), HMF (5 mM), **Ru$_4$**/PEI-rGO catalyst, reaction time (6 h), applied potential at 1.5 V vs RHE. [a] The amount of catalyst used in the electrocatalytic experiment, corresponding to the volumes of **Ru$_4$**/PEI-rGO catalyst ink supported by carbon cloth are 50, 75, 100, 125, 150, 200 μL.

Table S3 Comparation of the electrocatalytic oxidation of HMF to DFF using different noble metal-based electrocatalysts.

Catalyst	Conditions	Potential (V vs. RHE)	HMF (mM)	HMF Con. (%)	DFF Yie./Sel. (%)	Reaction time (h)	Ref.
Ru$_4$/PEI-rGO	0.5 M pH=6 NaAc/HAc	1.50	5	50.8	33.6/66.2	6	This work
PtRu	0.1 M H_2SO_4, 50°C	1.6 V vs. SHE	100	25.0	22.3/89.0	17	[1]
Pt/Fe_3O_4/rGO	0.1 M K_2SO_4	0.85 V vs. Ag/AgCl	0.5	7.2	6.8/94.4	20	[2]
Pt	1 M H_2SO_4, 60°C	2.00	20	88.3	13.1/14.8	100 C passed	[3]
Pb modified-Pt	0.1 M NaOH	0.90	10	100.0	50.4/80.0	2000 C passed	[4]
Pt foil	0.1 M NaOH	2.10	10	70.0	18.0/25.7	12	[5]

References

[1] T. Cao, M. Wu, V. V. Ordomsky, X. Xin, H. Wang, P. Métivier, M. Pera-Titus, *ChemSusChem* **2017**, *10*, 4851-4854.

[2] C. Zhou, W. Shi, X. Wan, Y. Meng, Y. Yao, Z. Guo, Y. Dai, C. Wang, Y. Yang, *Catalysis Today* **2019**, *330*, 92-100.

[3] S. R. Kubota, K.-S. Choi, *ChemSusChem* **2018**, *11*, 2138-2145.

[4] K. B. Kokoh, E. M. Belgsir, *Tetrahedron Letters* **2002**, *43*, 229-231.

[5] K. R. Vuyyuru, P. Strasser, *Catalysis Today* **2012**, *195*, 144-154.